

Benzamidine-based coatings: Implication of inhibitor structure on the inhibition of coagulation enzymes in solution and *in vitro* hemocompatibility assessment

Marie-Françoise Gouzy, Claudia Sperling, Katrin Salchert, Tilo Pompe, Cordula Rauwolf, and Carsten Werner^{a)}

Leibniz Institute of Polymer Research Dresden, Max Bergmann Center of Biomaterials Dresden, Hohe Str. 6, 01069 Dresden, Germany

(Received 14 September 2006; accepted 11 December 2006; published 31 January 2007)

Synthetic inhibitors of trypsin-like serine proteases were covalently immobilized to polymeric materials to passivate coagulation enzymes during blood contact. The inhibitory potency of a structurally simple and larger, more complex amidine derivatives was assessed against thrombin and factor Xa. After adsorption of serum albumin, the polymer films decorated with either one of the inhibitors were found to scavenge thrombin—with a higher affinity in the case of the larger inhibitor—but not factor Xa. Both inhibitor-containing coatings showed a significantly reduced thrombogenicity, coagulation activation, as well as complement activation when incubated with freshly drawn human whole blood *in vitro*. The authors conclude that the introduced principle offers a promising approach for hemocompatible materials for short term applications. Even rather simple inhibitors can be successfully employed for that purpose. © 2006 American Vacuum Society. [DOI: 10.1116/1.2431753]

I. INTRODUCTION

The application of blood-contacting medical devices often is limited by the activation of hemostatic mechanisms which are physiologically directed towards the prevention of blood loss from injured blood vessels.¹ One major consequence of the exposure of blood to almost any foreign material—as well as air—is the activation of thrombin and factor Xa (FXa), two key enzymes of the blood coagulation cascade. Thrombin, which is formed after the catalytic cleavage of its plasma precursor, prothrombin (factor II), through the tenase factor (FXa+FVa+Ca²⁺+phospholipid) converts fibrinogen into fibrin. Additionally it stimulates platelets with respect to expansion, aggregation, and release of components of the alpha and dense granules. Therefore, blood cell aggregates (thrombi) are formed on materials surfaces and microemboli (aggregate portions) might be liberated into the blood stream. The clots can induce a dysfunction of the medical devices, while the microemboli create the risk of harming the function of vital organs. The expressions of the bioincompatibility are variable and numerous: embolic complications with catheters,² thrombotic complications associated with a cardiovascular bypass,³ or occlusion of stents.⁴

To prevent these undesired blood responses, several strategies rely on the regulation of blood coagulation enzymes or passivation of the material surface. Enzyme activities might be turned off by loading biologically active substances into a polymer matrix or bonding them to the material surface. Commonly, these coatings are based on natural substances of mammalian origin: immobilization^{5–7} or release⁸ of anticoagulant sulfated polysaccharides (mainly heparin) or coat-

ings based on anticoagulant proteins as thrombomodulin.⁹ Beyond that hirudin,^{10,11} a nonmammalian protein preventing blood clotting was utilized to inhibit the functions of thrombin. Coatings with low thrombogenicity were also prepared by sustained release of a synthetic thrombin inhibitor from synthetic polymer matrices¹² and by covalent immobilization of a nonsteroidal anti-inflammatory drug,¹³ inhibitors of platelet activation, and aggregation¹⁴ or thrombin.^{15,16} On the other hand, materials passivated with polyethylene glycol molecules were reported as blood compatible cushions by minimizing and retarding the adsorption of plasma proteins as well as limiting the platelet adhesion.^{17–19} Other protein resistant surfaces relied on the surface decoration with phosphorylcholine.²⁰ Protein adsorption on both surfaces was essentially the same for similar chain length and density.²¹

While all of the above-listed principles were demonstrated to be successful in appropriate settings (as the commonly used systemic application of heparin), their utilization in order to gain hemocompatible medical devices remained so far rather limited. This limited translation of the previously developed strategies into practice provokes research towards more simple, defined, and robust anticoagulant coatings.

To address this challenge, we focus on the use of synthetic amidine derivatives described in literature as direct inhibitors of trypsin-like serine proteases (i.e., blood coagulation enzymes such as thrombin or factor Xa) but similarly of enzymes involved in the inflammation process such as complement C 1s.²² We already demonstrated that the covalent grafting of an amidine-containing inhibitor through reactive polymer films provides promising short term blood compatibility to the modified materials *in vitro*.²³ Optimization of the structure of the inhibitor, its linkage to the carrier mate-

^{a)}Author to whom correspondence should be addressed; electronic mail: werner@ipfdd.de

rial, and the overall physicochemical characteristics of the functionalized layer are assumed to allow further enhancement of the anticoagulant performance of the coatings.

In that context, the present study concerns the preparation and surface characterization of polymer coatings containing two different amidine-based molecules. Analyzing physicochemical characteristics of the inhibitor-decorated surfaces, their interactions with trypsin-like serine proteases in solution, and the biological response after contact with human whole blood, we show that the performance of amidine-based anticoagulant coatings is mainly controlled by the inhibitor structure.

II. MATERIALS AND METHODS

A. Amidine derivatives

4-aminobenzamidine dihydrochloride or inhibitor 1 was purchased from Aldrich-Fluka Chemicals (Deisenhofen, Germany) and used without further purification. *N* α -(2-naphthalenesulfonyl-L-lysyl)-4-amidino-DL-phenylalaninepiperidide ditrifluoroacetate or inhibitor 2 was synthesized with slight modifications of a published route.²⁴ The structure of the inhibitor 2 was confirmed by NMR (¹H and ¹³C) and mass spectroscopy (MALDI-TOF) (data not shown).

B. Details of the computational procedure

We applied the PM3 Hamiltonian,²⁵ in the form of the software package SPARTAN²⁶ using the WINDOWS2000 platform. The structures of the inhibitor molecules 1 and 2 were generated by the molecule editor and the energy was minimized without any constraints.

Thrombin is composed of two polypeptide chains *A* and *B* that are covalently linked through a disulfide bridge.²⁷ The *B* chain has the typical folded form of serine proteases²⁸ and involves the functional epitopes of the enzyme in a deep canyonlike binding site pocket on its molecular surface. In order to perform computational calculations it is necessary to restrict the large thrombin molecule. We focused on the relevant amino acid residues of the binding site pocket. Therefore, the atom coordinates of the thrombin binding site residues for the modeling studies were extracted from x-ray structure data of human α -thrombin from the Brookhaven Protein Data Bank.²⁹ The truncation points of residues were saturated with hydrogen.

For the semiempirical calculations the inhibitor moieties were placed into the binding site of thrombin and the energy of the complex was minimized, whereas the residues forming the thrombin active site were kept fixed. The binding strength of inhibitor-thrombin complexes $\Delta(\Delta H)$ was calculated.

C. Determination of the inhibitor potential

The inhibition of human thrombin and factor Xa was determined in 96 well plates using a chromogenic enzyme activity assay. All assays were carried out in a total volume of 200 μ l. Inhibitor dilutions (50 μ l) were incubated 5 min at

25 °C in 0.05 *M* tris buffer (Sigma-Aldrich Chemie GmbH, Steinheim, Germany) pH 7.4, containing 10% DMSO, 0.1 *M* NaCl, and 1 mg/ml bovine serum albumin (BSA) Sigma-Aldrich Chemie GmbH, Steinheim, Germany) with 100 μ l chromogenic substrate. The reactions were started with the addition of thrombin or factor Xa. The enzyme activities were evaluated from the hydrolysis rate of the substrates measured at 405 nm using a Genios spectrophotometer (Tecan, Austria GmbH, Grödig/Salzburg, Austria). The kinetic assays were performed over 20 min, in duplicate at three different inhibitor and six different substrate concentrations. The inhibition constant values (K_i) were determined using a direct Michaelis-Menten analysis. The calibration for the reaction product *para*-nitroaniline (*p*NA) (Sigma-Aldrich Chemie GmbH, Steinheim, Germany) was done using concentrations ranging from 0 to 200 μ M.

Enzyme and chromogenic substrate concentrations and supplier for each assay were as follows: human thrombin (T-6884, Sigma-Aldrich Chemie GmbH, Steinheim, Germany), at final concentration of 1.5 nM; thrombin-substrate H-D-Phe-Pip-Arg-*p*NA, 2HCl, or S-2238 (Chromogenix, Milano, Italy) at final concentrations between 0 and 300 μ M; factor Xa (Haemochrom Diagnostica GmbH, Essen, Germany) at final concentration of 0.7 nM; and FXa-substrate Z-D-Arg-Gly-Arg-*p*NA or S-2765 (Haemochrom Diagnostica GmbH, Essen, Germany) at final concentrations comprised ranging from 0 to 400 μ M.

D. Surface modification/inhibitor immobilization

Poly(propylene-*alt*-maleic anhydride) copolymer or PP-MA (MW=39 000, Leuna-Werke AG, Germany) was precipitated from tetrahydrofuran (Fluka, Deisenhofen, Germany) with hexane (Fluka), filtered out and thereafter intensively washed with hexane to remove olefin impurities. The reannulation of the anhydride moieties was completed at 120 °C for 20 h. Stable thin films of PP-MA were prepared by spin-coating a 0.1% copolymer solution in 2-butanone onto cleaned and amino-silanized silicon wafers or glass cover slips prepared according to the procedure described elsewhere.³⁰

The references utilized in this study were PP-MA films: first, the polymer films were freshly annealed (120 °C, 2 h) shortly before the experiment (PP-MA_{anh}) and, second, a total hydrolysis of the anhydride moieties of the copolymer film was achieved by autoclaving (120 °C, saturated water vapor, 20 min, autoclave: 2540 EL, Systec, Wettenberg, Germany) and led to a negatively charged surface PP-MA_{hyd}.

The immobilization of the inhibitors 1 and 2 was accomplished by direct modification of nonhydrolyzed thin films of PP-MA_{anh}: the copolymer films were immersed overnight in a 5 mM solution of the inhibitor in 0.1 *M* borate buffer (pH = 8) containing 10% DMSO, subsequently rinsed with deionized water and 0.01 *N* HCl solution, and annealed 2 h at 120 °C leading to the formation of the surfaces PP-MA-1 and PP-MA-2, respectively.

E. Physicochemical characterization

Layer thickness values were determined by ellipsometry using a single-wavelength device (632 nm) EL X-02C (DER Riss Ellipsometerbau GbmH, Ratzeburg, Germany). Coatings were performed in duplicate. The mean thickness of PP-MA films and modifications was determined from at least three measurements each and estimated using an optical 4 four-layers model (Si/SiO₂/polymer/ambient).³¹ The optical constants of Si (3.8705−*j*0.0168) and SiO₂ (1.4571 +*j*0.0000) layers were taken from literature.³² More details of the method and the analysis are given in Ref. 33. The refractive indices of the poly(alkene-*alt*-maleic anhydride) thin films were determined to be 1.5037 +*j*0.0000 by means of spectroscopic ellipsometry and kept invariant for the evaluation of the ellipsometry data of the modified layers. The given thickness values represent only the approximate change in film thickness since the intrinsic refractive indices of benzamidine-type inhibitors have not been determined yet.

Dynamic water contact angle measurements were carried out on an optical contact angle device OCA 30 (Dataphysics, Filderstadt, Germany). Droplets of Millipore water were, respectively, expanded and reduced with a velocity of 0.5 μl s^{−1} to obtain advancing and receding contact angles. The values are reported as average of three measurements.

X-ray photoelectron spectroscopy (XPS) was carried out using an Amicus spectrometer (Kratos Analytical, UK) equipped with a nonmonochromatic Mg Kα x-ray source operated at 12 kV and 240 W. The kinetic energy of photoelectrons was determined using an analyzer with a pass energy of 75 eV. The take-off angle, defined as the angle between sample surface normal and the electron optical axis of the spectrometer, was 0°. Spectra were referenced to the hydrocarbon C 1s peak at a binding energy of 285.00 eV. Quantitative elemental compositions were determined from the peak areas of the high resolution spectra (C 1s, N 1s, O 1s, S 2p, and Si 2p) using experimentally determined sensitivity factors and the spectrometer transmission function. The surface density of the inhibitors 1 and 2 was estimated from the elemental composition by a linear equation analysis assuming a density of 2.85 g cm^{−3} of the detected SiO₂ from the silicon wafer substrate and a mean attenuation length of the XPS signal in the substrate and the surface layer of about 3 nm.^{34,35} Within this routine the elemental compositions (C, N, S, and Si) of the layer components (SiO₂, PP-MA, PP-MA-1, or PP-MA-2) were fitted to the XPS data in a least square sense.

F. Serum albumin adsorption

Fluorescent labeled bovine serum albumin BSA-TRITC (tetramethylrhodamine isothiocyanate) was used as commercially available (Rockland, Gilbertsville, PA). Unlabeled BSA was purchased from Sigma (Sigma-Aldrich Chemie GmbH, Steinheim, Germany). For protein adsorption experiments, the polymer surfaces were immersed in a solution of serum albumin at a concentration of 250 μg ml^{−1} (mixture of

$\frac{1}{4}$ labeled to $\frac{3}{4}$ nonlabeled protein) in phosphate buffered saline (PBS) (Sigma-Aldrich Chemie GmbH, Steinheim, Germany) at pH 7.4 for 2 h. Fluorescence confocal laser scanning microscopy (TCS SP, Leica, Bensheim, Germany) was performed to reveal information from the plane of adsorption directly on the substrate surface. The experiments have been repeated twice. Laser intensities were calibrated prior to each measurement by using the InSpeck Orange calibration kit (Molecular Probes). The amount of immobilized serum albumin on the copolymer surfaces PP-MA_{anh} and PP-MA_{hyd} was quantified by HPLC-based amino acid analysis of the protein mixtures as described elsewhere.³⁶

G. Thrombin and factor Xa binding studies

The amounts of thrombin and factor Xa remaining in solution after contact with the modified surfaces were assayed using the chromogenic substrates S-2238 and S-2765, respectively. The reference surfaces PP-MA_{anh} and PP-MA_{hyd} and the test surfaces PP-MA-1 and PP-MA-2 were placed flat into customized screening chambers having a test-material area of 2 cm². The tested surfaces were incubated for 15 min with 200 μl PBS (pH 7.4) containing 10 mg/ml BSA and 0.1M NaCl. After incubation, the buffer solution was removed; thrombin (200 μl; 60 nmol l^{−1}) or factor Xa in PBS (200 μl; 60 nmol l^{−1}) in Tris buffer (pH 7.4, Sigma-Aldrich Chemie GmbH, Steinheim, Germany) were then added and equilibrated under agitation for 30 min at 25 °C. Then the supernatant solution was removed and diluted by a factor of 40 using tris buffer. 75 μl of this solution were incubated with chromogenic substrates (250 μM, 75 μl) in the wells of a 96-well microtiter plate for 60 min at 25 °C. The residual enzymatic activities were evaluated by measuring the amount of released *p*-nitroaniline at 405 nm at a reaction time *t*=25 min. The assays were performed twice, each time on five or six similar samples in parallel and reported normalized to the nonhydrolyzed PP-MA films PP-MA_{anh}.

The relative amounts of adsorbed enzyme on the surfaces were detected by immunostaining-fluorescence spectroscopy. After removal of the solution containing thrombin, the samples were rinsed three times with PBS. Afterwards, the samples were incubated for 1 h with a monoclonal anti-thrombin antibody (50 μg ml^{−1}, Acris, Bad Nauheim, Germany) followed by extensive rinsing (three times) with PBS. Thereafter, a TRITC labeled secondary antibody (1:50, donkey antishoop, Dianova, Hamburg, Germany) was incubated for 30 min. The surfaces were imaged using a confocal laser scanning microscope having a 40× oil immersion objective. The similar procedure was applied for the detection of adsorbed factor Xa using a primary mouse antihuman factor X IgG (American Diagnostica GmbH, Pfungstadt, Germany) and a TRITC labeled secondary antibody (1:50, donkey anti-goat IgG, Dianova, Hamburg, Germany).

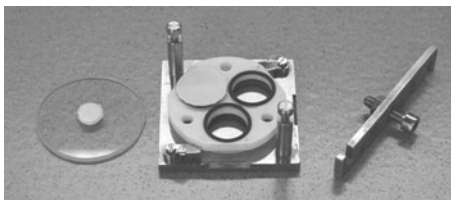


FIG. 1. Screening chamber for *in vitro* hemocompatibility assays. (Test-material area 6.3 cm²; blood volume filled in: approximately 2 ml.)

H. *In vitro* hemocompatibility assays

The generated materials were incubated with freshly drawn human blood. Briefly, whole human blood (60 ml) was drawn by venopuncture with a 19 gauge needle into two medical syringes (Braun, Melsungen, Germany) from a male healthy donor who did not take any medication for more than 10 days. Anticoagulation was achieved with heparin sodium salt grade 1-a (2 IU/ml) (H-3149 Sigma-Aldrich Chemie GmbH, Steinheim, Germany). The study was approved by the Ethics Committee of the Dresden University Hospital, Dresden, Germany. Informed consent was obtained from the donor before blood drawing. The assays were performed in duplicate, each time any marker being tested from three different samples. The blood was filled into the in-house built incubation chambers (Fig. 1) directly from the syringes. Incubation chambers modified after Ref. 37 with a test-material area of 6.3 cm², were filled with approximately 2 ml of blood avoiding the formation of air bubbles.

To reduce the sedimentation of blood cells during the incubation phase (2 h), the chambers were turned slowly by a rotary construction with an epicyclic gear which was placed in an incubator (B6030, Heraeus, Hanau, Germany) at 37 °C. Commercial enzyme-linked immunosorbent assays (ELISAs) were used to characterize the changes in activation markers for coagulation (thrombin-antithrombin complex, TAT), complement activation (complement fragment C5a), and thrombogenicity (platelet factor 4, PF4). ELISAs, used to quantify the latter substances, were purchased as follows: TAT (Enzygnost®TAT micro, DADE Behring Marburg, Germany), Zymutest PF4 (HYPHEN BioMed, Neuville sur Oise, France), and C5a (C5a-Micro DRG Diagnostica, Marburg, Germany). The ELISA plates were analyzed using an anthos 2010 photometer (Anthos Mikrosystems, Krefeld, Germany). Cell numbers (leukocytes, platelets, and erythrocytes) were analyzed by means of a blood analyzer (Coulter AcT_{diff}, Krefeld, Germany). The results are presented as the mean and standard deviation (SD).

I. Surface analysis of complement activation

The surfaces were rinsed carefully with veronal-buffered saline (Institut Virion, Rüschlikon/Zürich, Switzerland). Then, they were rinsed with distilled water to remove adherent salt and frozen at -70 °C until analysis. We used PBS containing 1% BSA and 0.1% Tween20 as working buffer and PBS containing 0.1% Tween 20 as washing buffer. Before analysis the surfaces were incubated with working

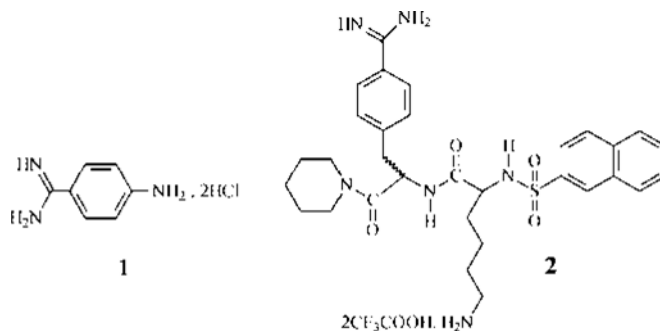


FIG. 2. Structure of the benzamidine-type inhibitors.

buffer for 15 min. Then the samples were incubated for 30 min with an antibody to C5b-9 (DAKO, Glostrup, Denmark) followed by a secondary antibody (DakoCytomatik, Hamburg, Germany) labeled with horse radish peroxidase. To quantify the bound antibody using a colorimetric reaction, the surfaces were incubated, after washing, for 20 min in the presence of 1,2-ortho-phenyldiamine dihydrochloride (Sigma-Aldrich Chemie GmbH, Steinheim, Germany). The reaction was stopped with 3M HCl and the adsorption read at 450 nm.

III. RESULTS AND DISCUSSION

Synthetic derivatives of benzamidine are described in the literature as direct inhibitors of trypsin-like serine proteases. Both the central enzymes of the blood coagulation cascade, thrombin and factor Xa, are sharing trypsin's preference for the binding of basic amino acid residues with Asp 189 present at the base of the primary specificity (S1) pocket of the enzyme. Due to their basic character, benzamidine (pKa=11.6)³⁸ and its derivatives are ligand (arginine)-mimicking molecules: the decoy molecules can bind the protease active center instead of its natural substrates. One example of such a structure is the thrombin inhibitor *N*α-(β-naphthylsulfonyl)glycyl-4-amidinophenyl-alanine piperidide (NAPAP) which is a result of extensive structure-activity relationship studies on piperidine amide derivatives of *N*α-arylsulfonyl benzamidine.³⁹

The structure of the two molecules, a small benzamidine derivative and a NAPAP analog, used for this study are displayed in Fig. 2. A structural prerequisite of the studied arginine-mimicking molecules is the presence of the primary amino group allowing for an effective attachment of the active compounds onto the reactive polymeric carrier. We worked with the commercial *p*-amino benzamidine (inhibitor 1), well known for its inhibitory activity of different serine proteases,¹⁶ and the inhibitor 2 in which the glycine of NAPAP was replaced by a lysine residue. Semiempirically calculated orientations of the molecules 1 and 2 to amino acid residues of the active site of thrombin are shown in Fig. 3.

The calculated orientations of inhibitors 1 and 2 in the thrombin binding site are in very good agreement with the experimental x-ray values of thrombin complexes with 4-aminobenzamidine⁴⁰ and NAPAP,⁴¹ respectively. The posi-

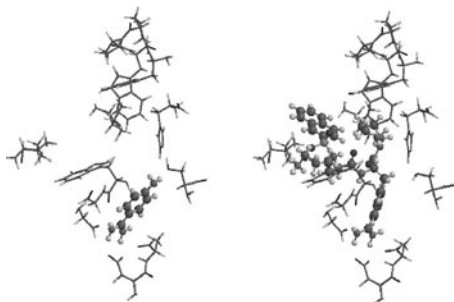


FIG. 3. Scheme of binding site orientation of the derivatives 1 (left) and 2 (right) to amino acid residues in thrombin active site.

tively charged benzamidine group of the inhibitors interacts with the acidic carboxylate group of the amino acid Asp189⁴² at the base of the catalytic pocket S1 and forms the typical ionic pair. The distances between the side chain of Asp189 and the benzamidine group of inhibitors 1 and 2 are 1.72 Å. In comparison to the small inhibitor 1 the branched inhibitor 2 completely fills the hydrophobic pockets S2 and S3 of the thrombin binding site. The length of the lysine residue of the inhibitor 2 is 5.6 Å, and it sticks out of the thrombin binding site.

The theoretically estimated differences in complex binding enthalpies $\Delta(\Delta H)$ are summarized in Table I. The thrombin-inhibitor complex structures are lower in energy than that of the separate molecules. The energetic stabilization of the inhibitor-thrombin complex results from favorable effects and interactions, e.g., hydrogen bonds, between the inhibitor molecules and the enzyme binding site.

The ability of these derivatives to inhibit thrombin and factor Xa in solution was measured using chromogenic substrate assays. The inhibition constants (K_i) are also summarized in Table I.

The experimental data showed that, in solution, the synthesized compounds are effective inhibitors of thrombin as well as of factor Xa. However, the *p*-aminobenzamidine (inhibitor 1) demonstrated a selectivity index (SI) factor Xa/thrombin of 0.06 while, as expected from modeling and literature data, the derivative 2 was highly selective against thrombin (SI=1025). The different SIs are easily explained by the structural differences existing between the active centers of the two enzymes: although strong similarities of the S1 specificity pockets (in which the amidine binding occurs) of the two enzymes exist, other subsites are showing distinct

TABLE I. Calculated heat of formation (PM3) of inhibitors, thrombin binding site residues, and inhibitor-thrombin complexes as well as inhibition constants against thrombin and factor Xa as determined by chromogenic assays.

	1	2	Thrombin
ΔH_{PM3} (kcal/mol)	175.9	232.1	-500.3
Thrombin complex:	-68.2	-117.9	...
$\Delta(\Delta H_{PM3})$ (kcal/mol)			
Thrombin: K_i (μ M)	422±54	0.08±0.03	...
Factor Xa: K_i (μ M)	26±10	82±28	...

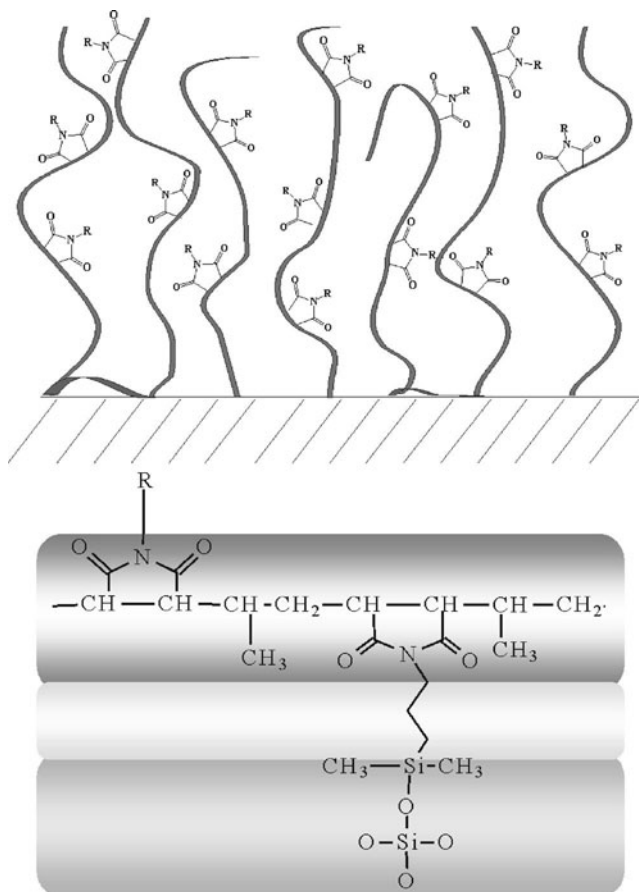


FIG. 4. Schemes of the inhibitor-modified polymer films where *R* represents one of the benzamidine-based inhibitors 1 and 2.

topologies. As an example, the hydrophobic subsite S2 in thrombin is smaller and only solvent accessible in factor Xa forcing benzamidine-based inhibitors to utilize two different conformations for the interaction with thrombin and factor Xa.⁴³ In our case, the hydrophobic naphthyl and piperidine substituents of 2 when stabilizing the thrombin-inhibitor 2 complex disadvantage the interactions with factor Xa.

A schematic representation of planar thin films of derivatized poly(propylene-*alt*-maleic anhydride) copolymers covalently attached to a solid support (silicon and glass coverslips) is displayed in Fig. 4 (bottom). Previous studies on the swelling behavior of such substrates before modification (i.e., bearing anhydride groups) revealed the formation of brush-like polymer layers resulting in a three-dimensional presentation of the reactive groups in the films [Fig. 4 (top)].⁴⁴ The principle of the surface immobilization of the synthetic inhibitor molecules is based on a nucleophilic reaction between the amino group present in the inhibitor and free surface anhydride groups of the polymer layer⁴⁵ generating a covalent link between the active moieties and the polymer surface. Inhibitor-modified surfaces were prepared with both inhibitors leading to the formation of PP-MA-1 and PP-MA-2. The reference substrates were annealed or hydrolyzed nonmodified polymer films reported as PP-MA_{anh} and PP-MA_{hyd}, respectively.

TABLE II. Change in film thickness values and atomic composition of inhibitor-modified PP-MA layers as determined by ellipsometry and XPS (at. %). The results are reported referenced to PP-MA_{anh}.

	Film thickness (nm)	C 1s (%)	O 1s (%)	N 1s (%)	Si 2p (%)	S 2p (%)
PP-MA _{anh}	3.1±0.4	53.4	32.7	0.5	13.4	0
PP-MA-1	+0.4±0.1	-2.7	-0.1	+1.9	+0.9	0
PP-MA-2	+2.4±0.4	+13.8	-11.4	+5.3	-8.2	+0.5

The substrate modifications were characterized with respect to changes in film thickness values, atomic composition of the polymer films (both listed in Table II), as well as surface wettability (reported in Table III). Analysis of the inhibitor treated surfaces demonstrated that a surface modification had occurred. The increase of the layer thickness values compared to the control indicated the attachment of the benzamidine-containing molecules.

Based on the elemental composition determined by x-ray photoelectron spectroscopy (Table II), the surface density of the immobilized molecules 1 and 2 was estimated as briefly outlined in Sec. II. For PP-MA-1 a lower surface density of $6 \times 10^{13} \text{ cm}^{-2}$ was found in comparison to a higher surface density of $2 \times 10^{14} \text{ cm}^{-2}$ for PP-MA-2.

A prepassivation of the surfaces with serum albumin can be considered as a model of the primary plasma protein adsorption phenomenon [i.e., the protein layer covering any material surface within seconds after contact with body fluid (blood/plasma/serum)].¹ The serum albumin adsorption data, at the chosen solution concentration of $250 \mu\text{g ml}^{-1}$ after 2 h of adsorption, are depicted in Fig. 5. HPLC-based amino acid analysis studies²⁸ which were made on the adsorption of serum albumin from a $250 \mu\text{g ml}^{-1}$ concentrated buffer solution onto the references PP-MA_{anh} and PP-MA_{hyd} substrate quantified the surface coverage of those surfaces by serum albumin at 0.32 ± 0.11 and $0.18 \pm 0.01 \mu\text{g cm}^{-2}$, respectively. A hypothetical monolayer of albumin molecules was calculated to be $0.24 \mu\text{g cm}^{-2}$.⁴⁶

Previous work demonstrated the effective tethering of proteins onto annealed maleic anhydride copolymer films through formation of an amide linkage between the surface anhydride groups and the ϵ -lysine side chains of the protein.⁴⁷⁻⁴⁹ The incubation of PP-MA_{anh} in the presence of serum albumin as also resulted in surface passivation due to the protein covalent attachment.

On the inhibitor-decorated surfaces (PP-MA-1 and PP-MA-2) the surface coverage by albumin is comparable to the situation on PP-MA_{hyd}. The surface coverage is reduced by a factor ~ 1.5 compared to PP-MA_{anh}.

TABLE III. Surface wettabilities. P=PTFE, G=glass.

	P ^a	G ^a	PP-MA _{hyd}	PP-MA-1	PP-MA-2
Advancing (°)	102	28	43±2	71±1	71±1
Receding (°)	88	35	31±1	42±1	40±1

^aReference 29.

The interactions of the blood coagulation enzymes (thrombin and factor Xa) with modified and nonmodified PP-MA substrates were characterized by determining the enzymatic activities of thrombin and factor Xa in solution after contact with the tested surfaces previously incubated in the presence of a serum albumin solution. In parallel the amount of adsorbed proteins was qualitatively evaluated by immunostaining/fluorescence spectroscopy. The collected data are shown in Figs. 6 and 7, respectively.

The lowest thrombin adsorption was observed on PP-MA_{anh} due to the covalent attachment of serum albumin and the resulting passivation of the surface. An enhanced thrombin adsorption was observed on PP-MA_{hyd}. In that case the blood coagulation enzyme was able to displace albumin and interact with the surface. The amount of adsorbed thrombin was increased when the inhibitor molecules were immobilized at the material surface suggesting that benzamidine-modified surfaces were able to adsorb thrombin with high affinity. Yet, a further increase of the antithrombin inhibitory strength of the immobilized molecule (PP-MA-2 versus PP-MA-1) manifests itself in the thrombin affinity of the surface {reduction of thrombin activity in solution [Fig. 6 (left)]} associated with an enhancement of enzyme adsorption at the material surface (Fig. 7).

Unlike thrombin, as seen in Fig. 6 (right) as well as in confocal laser scanning microscopy images (data not shown), no evidence of a binding of factor Xa onto the tested surfaces could be seen: we hypothesized that factor Xa was

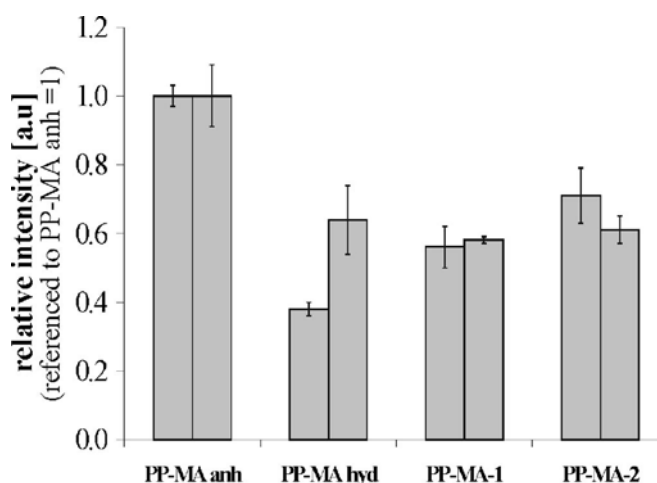


FIG. 5. Adsorbed serum albumin on modified and nonmodified substrates as determined by laser scanning microscopy.

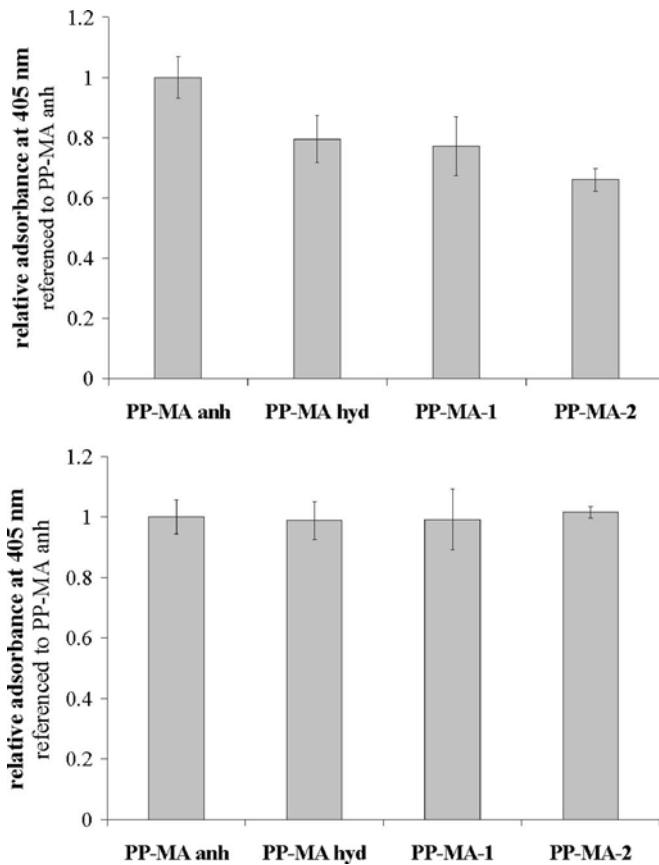


FIG. 6. Remaining enzyme activities in solution after contact with the inhibitor-modified and nonmodified PP-MA films: thrombin (top) and factor Xa (bottom). The results are reported referenced to PP-MA_{anh}. Each assay represents the average value of at least four single measurements.

not able to displace the preadsorbed albumin layer. An improvement of the hemocompatibility characteristics of these surfaces due to a factor Xa scavenging and inhibition could be ruled out.

To study the interaction of blood proteins and cells with the nonmodified materials PP-MA_{hyd} and inhibitor-

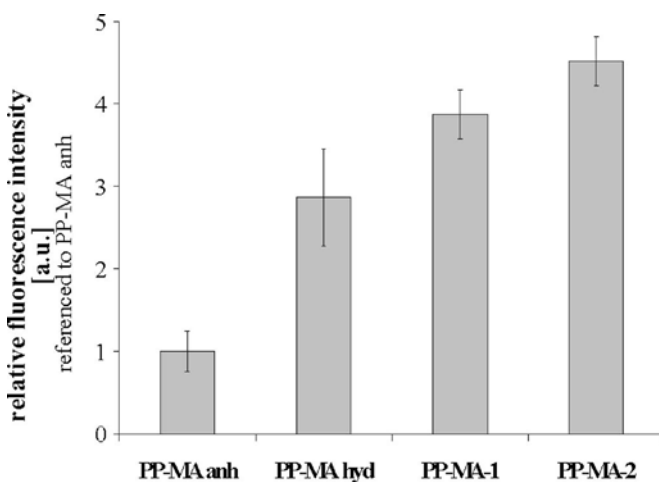


FIG. 7. Adsorption of thrombin on modified and nonmodified surface PP-MA substrates as determined by laser scanning microscopy.

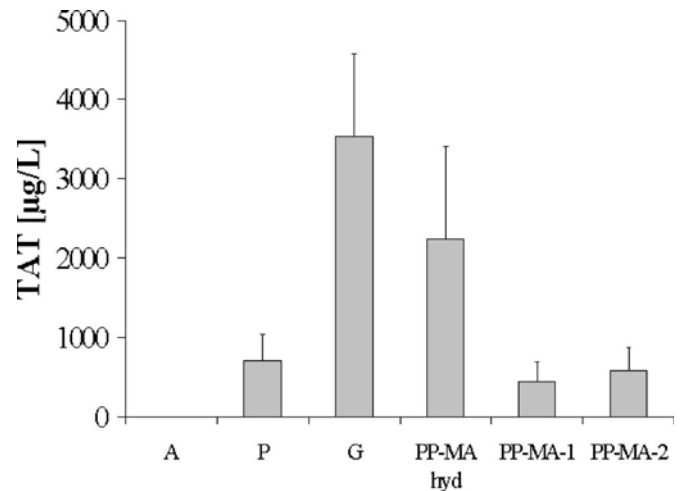


FIG. 8. Concentrations of TAT in blood plasma before (A) and after blood incubation with samples for 2 h. Reference materials: P=PTFE and G=glass. The error bars are standard deviations ($n=6$).

containing substrates, PP-MA-1 and -2, we investigated the changes in different activation markers, such as the blood cell number, activation of the coagulation cascade, complement system, and thrombocytes using dedicated incubation experiments with freshly drawn human whole blood. The customized incubation system is depicted in Fig. 1. The materials were compared using ELISAs for the following parameters: formation of the thrombin-antithrombin complex for coagulation activation (Fig. 8) and release of PF4 from the α -granula (one of the several platelet reactions after activation) (Fig. 9). Additionally, the number of thrombocytes in blood is compared between the samples in Table IV. The generated surfaces are referenced to A which is the value of the corresponding marker in human whole blood before incubation. A reference material P, poly(tetrafluoroethylene) (PTFE), which is extensively used in medical devices (more than 80% of vascular accesses in the United States being

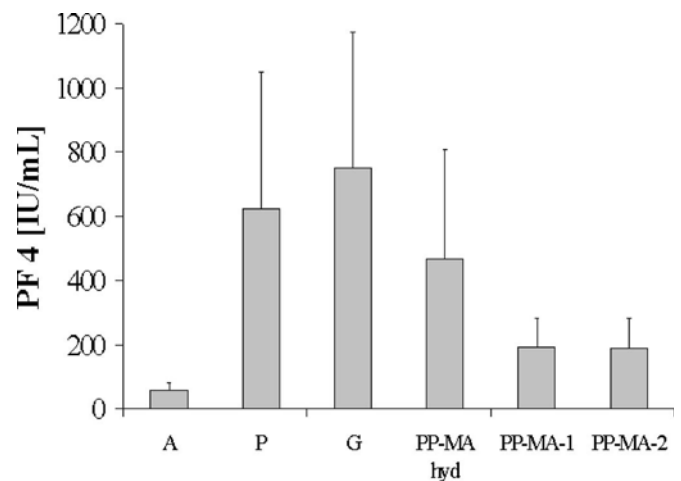


FIG. 9. Concentrations of PF4 in blood plasma before (A) and after blood incubation with samples for 2 h. Reference materials: P=PTFE and G=glass. The error bars are standard deviations ($n=6$).

TABLE IV. Number of thrombocytes in blood before (A) and after blood incubation with samples for 2 h ($n=5$). P =PTFE, G =glass. The results are shown as mean \pm standard deviation ($n=6$).

	A	P	G	PP-MA _{hyd}	PP-MA-1	PP-MA-2
Platelets $\times 10^9/l$	207	167	165	169	194	184
SD	5	12	16	21	9	11

expanded PTFE grafts) was included in the assay. Glass (G) was also chosen as reference due to its high procoagulant activity.

A strong formation of TAT was shown by PP-MA_{hyd} and glass. Being less hydrophilic than glass (as assessed by the surface wettability data depicted in Table III), PP-MA_{hyd} nevertheless exhibits a high density of negatively charged groups ($\sim 1 \times 10^{14}$ acid groups/cm²).²⁵ Negatively charged surfaces are known to initiate the contact activation of the blood coagulation system.⁵⁰ The drop in platelet number from the initial value of $(207 \pm 5) \times 10^9$ to (165 ± 16) and $(169 \pm 21) \times 10^9$ after the incubation with glass and PP-MA_{hyd}, respectively, confirms the fact that both are highly activating surfaces.

PP-MA-1 and PP-MA-2 surfaces displayed a significant decrease of the thrombocyte (PF4) and coagulation (TAT) activation markers compared to the nonmodified PP-MA_{hyd}: The immobilization of the two benzamidine-based inhibitors resulted in an observable decrease of the activation of the cascade systems. Yet, the slight differences between the two could not be considered as significant. The inhibitory strength (determined in solution) of the attached molecules, even if influencing the amount of scavenged thrombin as proved by the thrombin adsorption experiments (Figs. 5 and 6), cannot be considered as governing the compatibility of the surface with whole blood: the capability of PP-MA-1 to bind thrombin seems to be sufficient to ensure a reduction of the surface thrombogenicity and blood coagulation. The two inhibitor-functionalized surfaces demonstrated comparable antithrombogenic and anticoagulant effects referenced to the parameters obtained for the reference PTFE (TAT = $712 \pm 327 \mu\text{g l}^{-1}$ and PF4 = $622 \pm 428 \text{ IU ml}^{-1}$, respectively). Also, the platelet number in blood did not differ significantly between PP-MA-1 and -2, as illustrated in Table IV. Compared to the value in the blood before incubation, the decrease of the thrombocyte number after contacting these amidine-containing materials is only of 6% and 11% while about 20% of platelets disappeared after incubation in the presence of PTFE, glass, and PP-MA_{hyd}.

In vivo, the activation of the complement system is achieved via three different pathways (termed classical, lectin, or alternative) with three distinct triggers becoming identical beyond activation of C5. The activation of immunological reactions in blood after the contact with biomaterials was monitored through the detection of the formation of the complement fragment C5a (Fig. 10) which is one of the so-called anaphylatoxins having potent chemotactic ability for

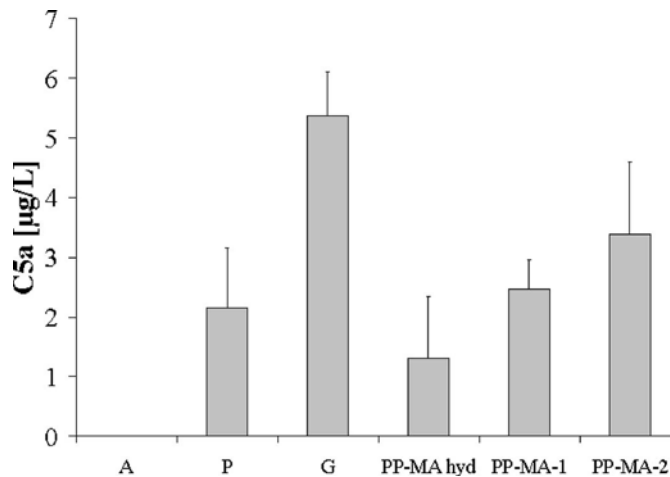


FIG. 10. Concentration of C5a in blood plasma before (A) and after blood incubation with samples for 2 h. Reference materials: P =PTFE and G =glass. The error bars are standard deviations ($n=6$).

polymorphonuclear cells and being an activator of monocytes and other leukocytes.⁵¹ Also, the formation of terminal complement complex C5b-9 or membrane attack complex which is common to the three pathways and capable of inserting into biological membranes and producing cell lysis and death (Fig. 11) was detected on the material surfaces. The complement activation associated with PP-MA-1 and PP-MA-2 was lower compared to the highly activating glass materials; however, low C5a production was observed as well after contact with hydrolyzed polymer films. It is known that negatively charged moieties such as COO^- (as in PP-MA_{hyd}) promote high-affinity association between the surface bound C3b and the inhibitory factor H inhibiting the further formation of complement system convertase. We consider the differences observed depending on the nature of the inhibitor which was immobilized at the surface as significant: lowest activation of immunological reactions in the blood as well as at the surface of the materials was noticed

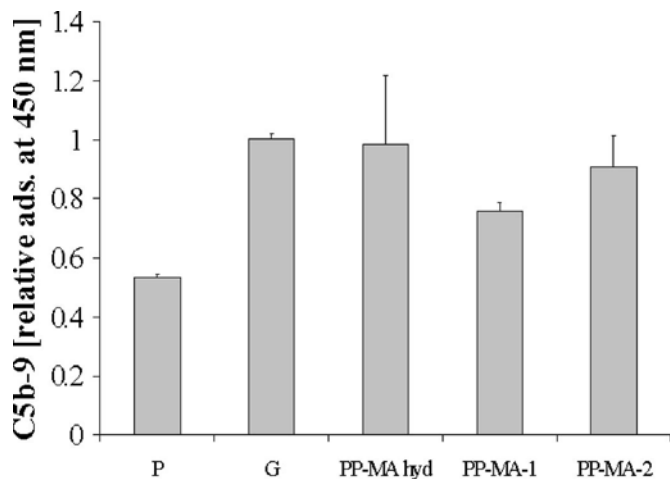


FIG. 11. Relative surface concentration of the terminal complement complex C5b-9 (results referenced to glass material, $G=1.0$). Reference materials: P =PTFE and G =glass. The error bars are standard deviations ($n=4$).

after contact with PP-MA-1 compared to PP-MA-2. As benzamidine molecules in solution are known to inhibit the complement fragment C1 competitively⁷ (the observed inhibition constant for the p-aminobenzamidine 1 were 1.35 and 0.4 mM for the serine proteases C 1s and C 1r, respectively),⁵² we assumed that such compatibility enhancement might be related to an inhibition of the first component of the complement system. It is usually assumed that the alternative pathway is responsible for the high activation noted on foreign surfaces.⁵³ However, *in vitro* results also supported the role of the first component of the classical pathway C1 in the activation of platelets.⁵⁴ Our results are in agreement with the new hypothesis that C1 is playing a role in the activation caused by foreign materials and that amidine-type agents could be effective due to their ability to inhibit subunits of this complement fragment.⁵⁵

IV. CONCLUSIONS

Our study demonstrates that the use of benzamidine-based molecules, inhibitors of trypsin-like serine proteases, offer a promising strategy for blood compatible coatings. Physicochemical and biological experiments prove the attachment and activity of benzamidine-type thrombin inhibitors on top of macroscopically flat surfaces precoated with reactive maleic anhydride copolymer thin films. The inhibitor-decorated polymer films scavenge thrombin even after a preincubation in the presence of serum albumin with an affinity related to the antithrombin potency of the molecules in solution. *In vitro* hemocompatibility parameters indicate that the immobilization of both synthetic inhibitors significantly enhanced the short term blood compatibility of the coatings. Both inhibitor decorated surfaces provided comparable antithrombotic and anticoagulant effects; the higher affinity of the larger inhibitor to thrombin was not reflected by the interaction of the coatings with human whole blood. Thus, even rather simple inhibitors can be successfully employed to design hemocompatible materials.

ACKNOWLEDGMENTS

The authors thank H. Komber and D. Voigt (both from the Leibniz Institute of Polymer Research Dresden) for carrying out NMR and MALDI-TOF measurements, respectively. The contributions of M. Nitschke, J. Huebner, G. Eberth, and A. Kuehn (Leibniz Institute of Polymer Research, Max Bergmann Center of Biomaterials) to this work are also gratefully acknowledged. This work was funded by the German Federal Ministry of Science and Education (Grant No. 03N4022: "BMBF Kompetenzzentrum für Materialien im Blut-und Gewebekontakt").

¹S. Hanson and B. D. Ratner, *Biomaterials Science*, edited by B. D. Ratner, A. S. Hoffman, F. J. Schoen, and J. E. Lemons (Academic, San Diego, 1996), pp. 228–238.

²R. C. Eberhart and C. P. Clagett, *Semin Hematol.* **28**, 42 (1991).

³G. P. Clagett and R. C. Eberhart, in *Hemostasis and Thrombosis: Basic Principles and Clinical Practice*, 3rd. ed., edited by R. W. Colman, J. Hirsh, V. J. Marder, and E. W. Salzman (Lippincott, Philadelphia, PA, 1994), pp. 1486–1505.

⁴J. A. Bittl, *J. Am. Coll. Cardiol.* **28**, 368 (1996).

⁵N. Weber, H. P. Wendel, and G. Ziemer, *Biomaterials* **23**, 429 (2002).

⁶R. M. Cornelius, J. Sanchez, P. Olsson, and J. L. Brash, *J. Biomed. Mater. Res.* **67A**, 475 (2003).

⁷R. de Vroeghe *et al.*, *Anesth. Analg.* (Baltimore) **98**, 1586 (2004).

⁸Y. B. Aldenhoff, M. L. Knetsch, J. H. Hanssen, T. Lindhout, S. J. Wielders, and L. H. Koole, *Biomaterials* **25**, 3125 (2004).

⁹C. Sperling, K. Salchert, U. Streller, and C. Werner, *Biomaterials* **25**, 5101S (2004).

¹⁰M. C. Wyers, M. D. Phaneuf, E. M. Rzucidlo, M. A. Contreras, F. W. LoGerfo, and W. C. Quist, *Cardiovasc. Pathol.* **8**, 153 (1999).

¹¹D. D. Kirn, M. M. Takeno, B. D. Ratner, and T. A. Horbett, *Pharm. Res.* **15**, 783 (1998).

¹²T. Richey, H. Iwata, H. Oowaki, E. Uchida, S. Matsuda, and Y. Ikada, *Biomaterials* **21**, 1057 (2000).

¹³G. A. Abraham, A. A. A. de Queiroz, and J. San Román, *Biomaterials* **23**, 1625 (2002).

¹⁴Y. B. J. Aldenhoff, F. H. van der Veen, J. ter Woorst, J. Habets, L. A. Poole-Warren, and L. H. Koole, *J. Biomed. Mater. Res.* **54**, 224 (2001).

¹⁵Y. Ito, L. S. Liu, R. Matsuo, and Y. Imanishi, *J. Biomed. Mater. Res.* **26**, 1065 (1992).

¹⁶X. Sun, H. Sheardown, P. Tengwall, and J. L. Brash, *J. Biomed. Mater. Res.* **49**, 66 (2000).

¹⁷P. Kingshott and H. J. Griesser, *Curr. Opin. Solid State Mater. Sci.* **4**, 403 (1999).

¹⁸W. R. Gombotz, W. Guanghui, T. A. Horbett, and A. S. Hoffman, *J. Biomed. Mater. Res.* **25**, 1547 (1991).

¹⁹J. H. Lee, H. B. Lee, and J. D. Andrade, *Prog. Polym. Sci.* **20**, 1043 (1995).

²⁰Y. Iwasaki and K. Ishihara, *Anal. Bioanal. Chem.* **381**, 534 (2005).

²¹W. Feng, S. Zhu, K. Ishihara, and J. L. Brasha, *BioInterphases* **1**, 50 (2006).

²²J. M. Andrews, D. P. Roman, and D. H. Bing, *J. Med. Chem.* **21**, 1202 (1978).

²³M.-F. Gouzy *et al.*, *Biomaterials* **25**, 3493 (2004).

²⁴T. Steinmetzer, A. Schweinitz, S. Künzel, P. Wikstroem, J. Hauptmann, and J. Stuerzebecher, *J. Enzyme Inhib.* **16**, 241 (2001).

²⁵J. J. P. Stewart, *J. Comput. Chem.* **10**, 209 (1989).

²⁶SPARTAN'02, Wavefunction, Inc., 2001.

²⁷E. Di Cera, Q. D. Dang, and Y. M. Ayala, *Cell. Mol. Life Sci.* **53**, 701 (1997).

²⁸A. M. Lesk and W. D. Fordham, *J. Mol. Biol.* **258**, 501 (1996).

²⁹G. De Simone *et al.*, *J. Mol. Biol.* **269**, 558 (1997).

³⁰T. Pompe, S. Zschoche, N. Herold, K. Salchert, M.-F. Gouzy, C. Sperling, and C. Werner, *Biomacromolecules* **4**, 1072 (2003).

³¹R. M. A. Azzam and N. M. Bashara, *Ellipsometry and Polarized Light* (Elsevier, Amsterdam, 1987), pp. 417–428.

³²J. A. Woollam, *User Manual VASE and M-44 Ellipsometers, WVASE 32TM* (J. A. Woollam, Lincoln, NE).

³³C. Werner, K. J. Eichhorn, K. Grundke, F. Simon, W. Grählert, and H. J. Jacobasch, *Colloids Surf., A* **156**, 3S (1999).

³⁴M. P. Seah and W. A. Dench, *Surf. Interface Anal.* **1**, 2 (1979).

³⁵D. A. Cole *et al.*, *J. Vac. Sci. Technol. B* **18**, 440 (2000).

³⁶K. Salchert, T. Pompe, C. Sperling, and C. Werner, *J. Chromatogr. A* **1005**, 113 (2003).

³⁷U. Streller, C. Sperling, J. Huebner, R. Hanke, and C. Werner, *J. Biomed. Mater. Res., Part B: Appl. Biomater.* **66B**, 379 (2003).

³⁸G. Hafelinger, in *The Chemistry of Amidines and Imidates*, edited by S. Patai (Wiley, New York, 1975), pp. 1–84.

³⁹J. Stuerzebecher, H. Vieweg, P. Wikstroem, D. Turk, and W. Bode, *Biol. Chem.* **473**, 491 (1992).

⁴⁰D. W. Banner and P. Hadvary, *J. Biol. Chem.* **266**, 20085 (1991).

⁴¹H. Brandstetter, D. Turk, H. W. Hoeffken, D. Grosse, J. Stürzebecher, P. D. Martin, B. F. P. Edwards, and W. Bode, *J. Mol. Biol.* **226**, 1085 (1992).

⁴²The numbering of amino acids of thrombin refers to chymotrypsin. Insertions relative to chymotrypsin are denoted by a letter: W. Bode, I. Mayr, U. Baumann, R. Huber, S. R. Stone, and J. Hofsteenge, *EMBO J.* **8**, 3467 (1989).

⁴³R. Rai, P. A. Sprengeler, K. C. Elrod, and W. B. Young, *Curr. Med. Chem.* **8**, 101 (2001).

⁴⁴T. Pompe, L. Renner, M. Grimmer, N. Herold, and C. Werner, *Macromol. Biosci.* **5**, 890 (2005).

⁴⁵U. Schmidt, S. Zschoche, and C. Werner, *J. Appl. Polym. Sci.* **87**, 1255

- (2003).
- ⁴⁶S. A. Sukhishvili and S. Granick, *J. Chem. Phys.* **110**, 10153 (1999).
- ⁴⁷C. G. Beddows, M. H. Gil, and T. Guthrie, *Biotechnol. Bioeng.* **28**, 51 (1986).
- ⁴⁸C. Ladaviere, T. Delair, A. Dormard, A. Novelli-Rousseau, B. Mandrand, and F. Mallet, *Bioconjugate Chem.* **9**, 655 (1998).
- ⁴⁹K. Salchert, U. Streller, T. Pompe, N. Herold, M. Grimmer, and C. Werner, *Biomacromolecules* **5**, 1340 (2004).
- ⁵⁰G. Tans, J. Rosing, and J. H. Griffin, *J. Biol. Chem.* **258**, 8215 (1983).
- ⁵¹R. M. Hakim, *Cardiovasc. Pathol.* **2**, 187S (1993).
- ⁵²S. S. Asghar, K. W. Pondman, and R. H. Cormane, *Biochim. Biophys. Acta* **317**, 539 (1973).
- ⁵³R. J. Johnson, in *Biomaterials Science*, edited by B. D. Ratner, A. S. Hoffman, F. J. Schoen, and J. E. Lemons (Academic, San Diego, 1996), pp. 173–187.
- ⁵⁴C. H. Gemmell, *J. Biomater. Sci., Polym. Ed.* **11**, 1197 (2000).
- ⁵⁵M. B. Gorbet and M. V. Sefton, *Biomaterials* **25**, 5681 (2004).